UDC 541.6:547.12

STRUCTURAL, ELECTRONIC, AND VIBRATIONAL PROPERTIES OF ACETYLENE ON Pd(100) DOPED WITH Sn OR Pb: A DFT CLUSTER MODEL STUDY

P. Matczak

Department of Theoretical and Structural Chemistry, University of Łódź, Łódź, Poland
E-mail: p.a.matczak@gmail.com

Some structural, electronic, and vibrational properties of the acetylene (C_2H_2) molecule adsorbed at various sites on the Pd(100) surface doped with Sn or Pb are determined theoretically. The calculations were performed using the B3LYP hybrid density functional, and the Sn- or Pb-doped Pd(100) surfaces were represented by a cluster model approach. It is found that the geometry of the C_2H_2 molecule adsorbed in di-σ configurations is highly perturbed with respect to the structure of acetylene in the gas phase. By contrast, the geometry of acetylene adsorbed in π configurations on the doped surfaces shows a much smaller distortion. Apart from calculating the properties of the adsorbed C_2H_2 molecule, the effect of the dopants, i.e. Sn and Pb atoms, on these properties is established by comparing the properties of acetylene adsorbed on the Sn- or Pb-doped Pd(100) surfaces with its properties on the monometallic Pd(100) surface. The results indicate that the geometry of the adsorbed C_2H_2 molecule is similar on the doped and monometallic Pd(100) surfaces.

K e y w o r d s: acetylene adsorption, Pd—Sn catalyst, Pd—Pb catalyst, DFT.

INTRODUCTION

In the petrochemical industry, cracking processes are used extensively to produce unsaturated hydrocarbons [1—3]. In the case of ethylene obtained by steam cracking, the cracker stream contains several percents of acetylene as a byproduct. This byproduct needs to be removed to avoid catalyst poisoning in some downstream processes, e.g. polymerization [4, 5]. The removal of acetylene from the ethylene stream is achieved through the selective hydrogenation of C_2H_2 to C_2H_4.

Palladium is the most selective and widely used metallic catalyst of acetylene hydrogenation [2, 3]. Its ability to carry out the C_2H_2 hydrogenation to C_2H_4 can be further improved by adding a second metal, i.e. a dopant, and forming a bimetallic catalyst. Various metallic dopants have been proposed, e.g. Sn [6, 7] and Pb [6, 8—10].

Acetylene adsorption on the surface of a palladium catalyst constitutes an important step of the selective hydrogenation to ethylene. The determination of various properties of the C_2H_2 molecule adsorbed on so-called model Pd catalysts, i.e., on the low Miller index surfaces of Pd, is necessary to provide an insight into the mechanism of the selective hydrogenation. However, many structural and electronic properties of the adsorbate on the catalyst surface may be difficult to measure experimentally. By contrast, computational chemistry allows for the relatively straightforward and reliable determination of such information [11, 12].

Theoretical studies of the acetylene adsorption on Pd catalysts are limited mainly to the (111) surface [13—18]. For the Pd(100) surface, Duca *et al.* [19] have investigated the lateral interaction between two acetylene molecules and found that this interaction is repulsive at all distances. The adsorption of acetylene on the Pd surfaces doped with Pb has been the subject of two computational studies

[20, 21]. Ferullo *et al.* [20] have carried out semiempirical calculations for C_2H_2 on the $Pd_3Pb(111)$ surface and their calculations indicate a strong negative effect of Pb atoms on the strength of the C_2H_2 adsorption on this surface. Very recently, García-Mota *et al.* [21] have provided the density functional theory (DFT) description of the C_2H_2 adsorption on the PdPb(111) surface. To the best of our knowledge, the adsorption of acetylene on Pd doped with Sn has not been investigated theoretically so far.

In the present work, we report the results of DFT calculations for the adsorption of acetylene on the Pd(100) surface doped with Sn or Pb. Some structural, electronic, and vibrational properties of the C_2H_2 molecule adsorbed on the Sn- or Pb-doped Pd(100) surfaces were calculated for various adsorption sites. The effect of the Sn and Pb dopants on the acetylene adsorption is also established by comparing the adsorbate properties on the doped (100) surfaces with those on the monometallic Pd(100) surface.

METHOD

We conducted quantum chemical calculations employing DFT implemented in the GAUSSIAN 09 suite of programs [22]. The chosen DFT method, namely the hybrid B3LYP density functional [23], was combined with the LANL08 basis set [24] for Pd, Sn, and Pb atoms and with the 6-311++G** basis set [25] for H and C atoms. The LANL08 basis set was supplemented with polarization functions [26]. This basis set is a revised version of the well-known LANL2DZ basis set [27]. The B3LYP functional, in conjunction with the LANL2DZ and the Pople-type basis set, was previously employed in the investigations of ethylene adsorption on Pd(100) [28] and PdSn(111) [29].

The interaction of the C_2H_2 molecule with the (100) surfaces of palladium and palladium doped with tin or lead was investigated using a cluster model approach. We decided to represent the investigated surfaces by means of 14-atom clusters, even though smaller clusters proved to be useful [28, 29]. The Pd(100) surface was modeled by the Pd_{14} cluster that comprised three layers containing 9, 4, and 1 metal atoms. The bimetallic clusters were formed by replacing a single Pd atom from the surface 9-atom cluster layer or from the subsurface 4-atom cluster layer with a Sn or Pb atom. For these clusters the distance from the nearest neighbor was equal to the value of the Pd bulk, namely 2.7512 Å. The Sn-doped Pd clusters $Pd_{13}Sn$ are denoted further in the text as PdSn(100), while the Pb-doped ones $Pd_{13}Pb$ as PdPb(100).

For the (100) surfaces of metals having the fcc crystal structure, three characteristic adsorption sites (namely, atop, bridge, and hollow ones) are usually considered in the studies of adsorbate-surface interactions. In the case of the PdSn(100) and PdPb(100) surfaces modeled in this work by the $Pd_{13}Sn$ and $Pd_{13}Pb$ clusters, the picture of adsorption is more complicated than that on the monometallic Pd(100) surface, since the second metal atom can be a part of an adsorption site or can be situated in the neighborhood of an adsorption site. Moreover, a dopant atom can occupy a place either in the surface layer or in the subsurface layer. For this reason, each of three characteristic adsorption sites is categorized into two variants, depending on the location of a dopant atom. An adsorption site that either contains or is adjacent to a surface dopant atom is denoted by the suffix I, whereas a site that has in its immediate proximity a subsurface dopant atom is marked with the suffix II (Fig. 1). Since we focus on the Pd sites doped
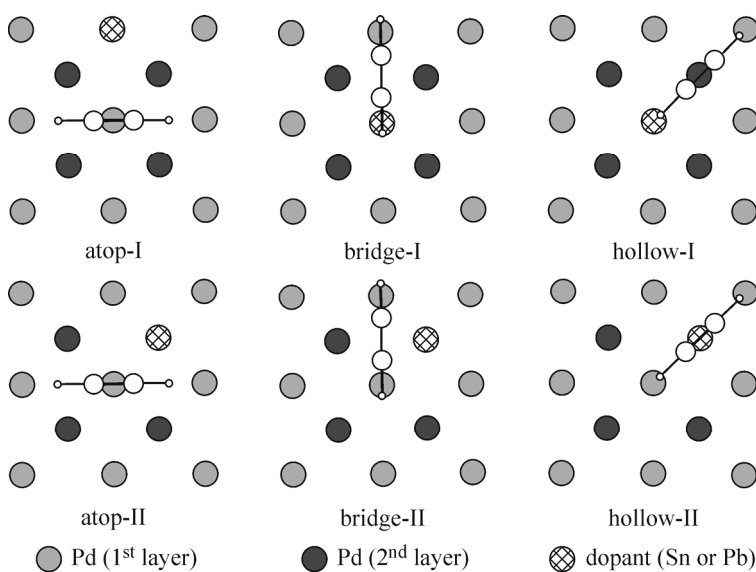

Fig. 1. Top views of the clusters representing the Sn- or Pb-doped Pd(100) surfaces with the C_2H_2 molecule adsorbed at the sites considered in this work

with a second metal, the adsorption of the C_2H_2 molecule at the atop site directly on a dopant atom was not studied.

The geometry of the acetylene molecule adsorbed at the considered sites on Pd(100), PdSn(100), and PdPb(100) was optimized using analytic gradients. In the course of the optimizations, two approaches were considered for the 14-atom clusters representing the (100) surfaces. In the first one, the clusters were assumed to keep the fixed crystal structure, whereas in the second, they were allowed to relax partially (the position of the metal atom in the center of the surface 9-atom layer could change).

It is known that cluster models of the surface are not suitable to determine reliably the adsorption energy. For this reason, the focus of this work is not on the adsorption energy of acetylene on PdSn(100) and PdPb(100), but rather on its adsorption properties such as geometrical parameters, electron charge transfers, and vibrations. All vibrational frequencies were scaled by a factor of 0.9679. This single scale factor was proposed by Andersson and Uvdal [30] to obtain fundamental vibrations from harmonic frequencies calculated at the B3LYP level of theory with basis sets larger than 6-311G**.

RESULTS AND DISCUSSION

The results calculated for the adsorption of the C_2H_2 molecule on the PdSn(100) surface are listed in Table 1. The distance d was measured between the center of the C—C bond of the adsorbed C_2H_2 molecule and the PdSn(100) surface (when partial relaxation was allowed, the distance was referenced to the level specified by the frozen atoms of the surface layer). For both variants of three considered adsorption sites the d values decrease in the series: atop > bridge > hollow. The order of this series can be associated with the fact that the more atoms of the surface are involved in the interaction with the adsorbate molecule, the closer to the surface this molecule sits. Within the framework of the frozen surface approach, acetylene adsorbs considerably closer to the surface at the atop-I site than it does at the atop-II one. By contrast, the bridge-I and hollow-I sites have greater d values, compared to those of their II variant counterparts. For the partially relaxed PdSn(100) surface all the adsorption sites in their I variant exhibit smaller d values than those of the corresponding sites in their II variant. In this case, however, the effective height of the C_2H_2 molecule from the surface is sometimes different from the corresponding d value. The vertical displacement Δz of the metal atom in the center of the cluster surface layer with respect to the adjacent frozen atoms reflects the influence of the adsorbate on the surface. Positive values of Δz indicate that the metal atom is elevated above the (100) surface, whereas negative ones show that the metal atom approaches the subsurface layer. With the Δz values taken into consideration, the effective distance of the C_2H_2 molecule from the surface is smaller only for the adsorption at the atop-I site, compared to that at the atop-II one. This remains in line with the result obtained for the acetylene molecule on the frozen PdSn(100) surface. When the C_2H_2 molecule approaches the PdSn(100) surface at the bridge-I, hollow-I, and atop-II sites, it induces negligible changes in the position of the surface metal atom. By contrast, the adsorption at the atop-I, bridge-II, and hollow-II sites leads to the significant relaxation of PdSn(100) and the surface metal atom is elevated by 0.2—0.3 Å.

The C_2H_2 molecule lies flat on the PdSn(100) surface only when adsorbed at the atop-I site. It results from the orientation of the molecule with respect to the dopant atom and from the symmetry of this adsorption site within our cluster model representing the (100) surface. As indicated by the $\angle$(C—C—surface) angle, the adsorption at the other sites brings about a small inclination of the molecular axis of C_2H_2 towards the surface. For the adsorption at the bridge-I and hollow-I sites, the C atom adjacent to the Sn dopant is placed noticeably higher from the surface than the other C atom and, therefore, the $\angle$(C—C—surface) values are greater than those of the atop-II, bridge-II, and hollow-II sites.

As for the geometry of the C_2H_2 molecule, its distortion induced by the adsorption on PdSn(100) can be found. The C—C bond length R(C—C) increases and the C—C—H angles ($\angle$C—C—H) bend upwards. The C—H bond lengths R(C—H) are also listed in Table 1. The C_2H_2 molecule adsorbed at all adsorption sites, except the atop-I one, is not symmetric and its two C—H bond lengths and/or two C—C—H angles are not identical. Therefore, Table 1 contains two values of R(C—H) and $\angle$(C—C—H).

T a b l e 1

Structural, electronic, and vibrational properties of the acetylene molecule adsorbed at the characteristic sites on the PdSn(100) surface. All the symbols are explained in the text. The values obtained for the partially relaxed surface are typed without parentheses, whereas those for the frozen surface are bracketed

Property	Adsorption site					
	atop-I	bridge-I	hollow-I	atop-II	bridge-II	hollow-II
d, Å	2.396	1.926	1.605	2.443	1.962	1.655
	(2.151)	(1.949)	(1.658)	(2.481)	(1.872)	(1.571)
$\angle$(C—C—surface), deg.	0.0	7.5	6.2	0.9	5.8	3.0
	(0.0)	(7.2)	(7.2)	(0.6)	(1.0)	(0.8)
R(C—C), Å	1.238	1.320	1.351	1.229	1.298	1.321
	(1.237)	(1.319)	(1.347)	(1.211)	(1.296)	(1.322)
R(C—H), Å	1.068	1.087	1.091	1.066	1.087	1.093
		1.091	1.097	1.067	1.085	1.093
	(1.067)	(1.087	(1.090	(1.064	(1.084	(1.092
		1.090)	1.097)	1.063)	1.086)	1.092)
$\angle$(C—C—H), deg.	160.2	126.6	119.4	162.8	133.6	124.3
		128.8	120.0	164.5	133.6	125.0
	(159.3)	(127.6	(120.2	(172.7	(134.3	(124.3
		129.6)	120.7)	174.4)	134.7)	125.8)
$\delta_{C—C}$, Å	0.039	0.121	0.152	0.030	0.099	0.122
	(0.038)	(0.120)	(0.148)	(0.012)	(0.097)	(0.123)
$\delta_{C—C—H}$, deg.	19.8	53.4	60.6	17.2	46.4	55.7
		51.2	60.0	15.5	46.4	55.0
	(20.7)	(52.4	(59.8	(7.3	(45.7	(55.7
		50.4)	59.3)	5.6)	45.3)	54.2)
Q_{MPA}, e	0.0145	–0.3996	–0.3870	0.1088	–0.0898	–0.0316
	(0.0735)	(–0.3806)	(–0.3632)	(0.1900)	(–0.1087)	(–0.0433)
Q_{NPA}, e	0.0932	–0.5682	–0.7358	0.1285	–0.0855	–0.2312
	(0.1058)	(–0.4387)	(–0.5702)	(–0.0017)	(–0.2646)	(–0.4677)
ν(C—H) sym, cm^{-1}	3317	3039	2995	3341	3076	2994
	(3314)	(3045)	(3002)	(3386)	(3088)	(3003)
ν(C—H) asym, cm^{-1}	3247	2989	2921	3266	3033	2966
	(3245)	(2996)	(2922)	(3296)	(3043)	(2975)
ν(C—C), cm^{-1}	1781	1472	1380	1826	1528	1471
	(1780)	(1470)	(1393)	(1923)	(1538)	(1462)
Δz, Å	0.303	0.038	–0.030	–0.044	0.238	0.222
	(0.000)	(0.000)	(0.000)	(0.000)	(0.000)	(0.000)

It is convenient to contrast the structural properties of the adsorbed C_2H_2 molecule with the geometry of free gas-phase acetylene. The differences in the C—C bond length and in the C—C—H angles between the free molecule and the adsorbed one are denoted in Table 1 as $\delta_{C—C}$ and $\delta_{C—C—H}$ respectively. The greater the values of $\delta_{C—C}$ and $\delta_{C—C—H}$ are, the more perturbed the C_2H_2 geometry becomes in the adsorption process. The smallest changes in the C_2H_2 geometry can be found for the atop-I and atop-II sites. The molecule combined with these sites corresponds to the π configuration that is characterized by the nearly unperturbed geometry of C_2H_2. By contrast, the acetylene adsorption at both variants of the bridge and hollow sites significantly distorts the adsorbate structure. For these sites the changes in the C_2H_2 geometry indicate a rehybridization of carbon atoms from sp towards sp^2. The most significant distortion of the C_2H_2 structure is observed for the hollow-I site. The calculated C—C—H angles

for acetylene at this site are practically 120°, which means that C atoms reach the sp^2 hybridization. The elongation of the C—C bond and the bends of the C—H ends suggest the structural similarity of the adsorbed species with the ethylene molecule (obviously with two H atoms missing). The resulting sp^2 hybrid orbitals are not fully saturated, enabling the C atoms to bind with the surface. The presence of the surface Sn dopant at the adsorption sites gives a more perturbed C_2H_2 geometry than the corresponding sites in the II variant do.

The partial relaxation of the PdSn(100) surface has a negligible effect on the geometry of the adsorbed C_2H_2 molecule, although the atop-II site seems to be an exception. The C_2H_2 molecule exhibits an almost unperturbed structure at the atop-II site on the frozen PdSn(100) surface, while its structural changes at this site on the partially relaxed surface are similar to those observed at the atop-I site.

The electron charge transfer between the adsorbate and the surface is investigated by means of the charge gathered by the adsorbed C_2H_2 molecule. This charge was calculated using the Mulliken population analysis [31] (Q_{MPA}) and the natural population analysis [32] (Q_{NPA}). The sign of the charge developed by the C_2H_2 molecule can be interpreted in terms of the Dewar—Chatt—Duncanson model of orbital interaction [33, 34]. According to this model, HOMO of the adsorbing C_2H_2 molecule can hybridize with the orbitals of surface metal atoms, resulting in electron donation from the adsorbate to the surface. This transfer is accompanied by electron charge back-donation from the occupied orbitals of surface metal atoms to adsorbate LUMO. In the case of C_2H_2 adsorbed at the atop-I and atop-II sites, the charge transfer is very small and the charge donation outweighs the back-donation, which is reflected by the positive values of Q_{MPA} and Q_{NPA}. The negative value of Q_{NPA} for the atop-II site on the frozen surface is sufficiently small to assume that the natural population analysis predicts no charge transfer in this case. By contrast, for both variants of the bridge and hollow sites the back-donation predominates, resulting in the negative Q_{MPA} and Q_{NPA} values. The bridge-I and hollow-I sites exhibit much more pronounced charge transfers from the surface to the C_2H_2 molecule than their II variant counterparts.

The frequencies of C—C and C—H stretching vibrations were calculated for the C_2H_2 molecule adsorbed at all the adsorption sites, and the results are shown in Table 1. The ν(C—C) stretching frequency is the lowest for the acetylene molecule bound with the hollow-I site, which indicates a significant distortion of the C—C bond (ν(C—C) of free gas-phase C_2H_2 amounts to ca. 1975 cm^{-1} [35]) and, in consequence, a weakening of the C—C bond strength. This is in agreement with the rehybridization of the C atoms from sp to sp^2 and the transition from a triple to a double C—C bond.

The calculated structural, electronic, and vibrational properties of the acetylene molecule adsorbed on the PdPb(100) surface are given in Table 2. The C_2H_2 molecule is adsorbed at the height from the surface that decreases in the sequence: atop > bridge > hollow. This sequence remains valid for the sites in both variants. The d values of the bridge-I and hollow-I sites are larger than those of their counterparts with the subsurface Pb dopant. The larger d values for the bridge-I and hollow-I sites can be seen irrespective of the fact whether the partial relaxation was allowed or not. It should be stressed that the partial relaxation of the PdPb(100) surface (expressed by Δz) is evident for all the adsorption sites. Of the Δz values in Table 2, that of the hollow-I site is the smallest, $\Delta z = 0.139$ Å. The greatest vertical displacements of the surface atom occur for the atop-I and atop-II sites. For the latter the replacement of the dopant atoms, i.e., Sn by Pb, causes a dramatic increase in the Δz value. It is worth noting that a rather high Δz value of 0.227 Å has also been reported for Pb atoms on the PdPb(111) surface [21].

The axis of the C_2H_2 molecule interacting with the atop-I site is parallel to the PdPb(100) surface. The adsorption at the bridge-I and hollow-I sites most inclines the adsorbate axis. It is worth noting that these sites on the PdPb(100) surface yield larger $\angle$C—C—surface values than the corresponding sites on PdSn(100).

The $\delta_{C—C}$ and $\delta_{C—C—H}$ parameters in Table 2 show that the geometry of C_2H_2 on PdPb(100) differs from that in the gas phase. For each location of the Pb dopant the growing distortion of the C_2H_2 geometry is seen for the adsorption sites in the following order: atop < bridge < hollow. Moreover, the sites with the surface Pb atom are able to perturb the structure of acetylene slightly more effectively

T a b l e   2

Structural, electronic, and vibrational properties of the acetylene molecule adsorbed at the characteristic sites on the PdPb(100) *surface. See the caption of Table 1 for further notes*

Property	Adsorption site					
	atop-I	bridge-I	hollow-I	atop-II	bridge-II	hollow-II
d, Å	2.449	2.036	1.719	2.456	1.969	1.660
	(2.107)	(1.991)	(1.706)	(2.509)	(1.870)	(1.570)
$\angle$(C—C—surface), deg.	0.0	12.6	9.3	0.9	6.3	3.0
	(0.0)	(9.0)	(7.8)	(0.3)	(0.8)	(1.2)
R(C—C), Å	1.244	1.311	1.333	1.230	1.299	1.320
	(1.245)	(1.311)	(1.333)	(1.210)	(1.296)	(1.322)
R(C—H), Å	1.069	1.085	1.088	1.066	1.086	1.093
		1.090	1.098	1.067	1.087	1.093
	(1.069)	(1.085	(1.088	(1.064	(1.084	(1.092
		1.090)	1.098)	1.063)	1.086)	1.092)
$\angle$(C—C—H), deg.	157.5	131.3	123.6	163.0	133.4	124.4
		129.5	121.8	164.5	133.3	124.9
	(155.1)	(131.3	(123.6	(173.4	(134.2	(124.4
		129.5)	121.8)	174.9)	134.7)	126.0)
$\delta_{C—C}$, Å	0.045	0.112	0.134	0.031	0.100	0.121
	(0.046)	(0.112)	(0.134)	(0.011)	(0.097)	(0.123)
$\delta_{C—C—H}$, deg.	22.5	48.7	56.4	17.0	46.6	55.6
		50.5	58.2	15.5	46.7	55.1
	(24.9)	(48.7	(56.4	(6.6	(45.8	(55.6
		50.5)	58.2)	5.1)	45.3)	54.0)
Q_{MPA}, e	−0.0772	−0.4707	−0.3955	0.1158	−0.0781	−0.0104
	(−0.0094)	(−0.4059)	(−0.3581)	(0.1937)	(−0.0977)	(−0.0165)
Q_{NPA}, e	0.0256	−0.4896	−0.6286	0.1266	−0.0906	−0.2343
	(0.0667)	(−0.3514)	(−0.4682)	(−0.0008)	(−0.2653)	(−0.4683)
v(C—H) sym, cm^{-1}	3300	3058	3018	3341	3074	2993
	(3294)	(3066)	(3028)	(3388)	(3087)	(3003)
v(C—H) asym, cm^{-1}	3235	2990	2915	3266	3032	2965
	(3232)	(3001)	(2923)	(3297)	(3044)	(2976)
v(C—C), cm^{-1}	1756	1484	1424	1824	1524	1473
	(1743)	(1487)	(1425)	(1928)	(1537)	(1465)
Δz, Å	0.394	0.218	0.139	0.309	0.265	0.247
	(0.000)	(0.000)	(0.000)	(0.000)	(0.000)	(0.000)

than the sites in the II variant. The inclusion of the partial relaxation of PdPb(100) in the calculations yields the C_2H_2 structures that are very similar to those obtained for the frozen surface. The effect of the partial relaxation of PdPb(100) on the adsorbate geometry is pronounced only in the case of the atop-II site. The same appeared for the PdSn(100) surface.

The comparison of the $\delta_{C—C}$ and $\delta_{C—C—H}$ values for acetylene on PdSn(100) and on PdPb(100) reveals that for each site in the II variant the structural distortion of the C_2H_2 molecule is practically the same for both dopants. More evident differences in the C_2H_2 geometry on the two surfaces occur for the sites with the dopants in the surface layer. The geometric structure of acetylene is slightly more perturbed at the atop-I site on PdPb(100) than at this site on PdSn(100). By contrast, the Pb dopant in the bridge-I and hollow-I sites shows a weaker ability to distort the acetylene geometry than the Sn dopant does.

As it is illustrated by Q_{MPA} and Q_{NPA} in Table 2, considerable charge transfers, together with the domination of back-donation, take place for the C_2H_2 molecule adsorbed at the bridge-I and hollow-I sites on PdPb(100). The adsorption at the other sites is accompanied by smaller charge transfers between the adsorbate and the surface. In particular, the charge of the C_2H_2 molecule at the atop-I site is very close to zero.

The analysis of the C—C stretching frequencies on PdPb(100) points out that the acetylene adsorption at the hollow-I site most distorts and weakens the C—C bond. For each site the weakening of the triple C—C bond character is more pronounced when the Pb atom is located in the surface layer.

In order to establish the influence of the dopants on the properties of the adsorbed C_2H_2 molecule, it is necessary to compare the results calculated for the acetylene adsorption on the doped surfaces with those on the monometallic Pd(100) surface. In the case of the acetylene adsorption on Pd(100), some experimental findings have been reported [35—37]. Acetylene adsorbs nondissociatively at room temperature on Pd(100) and its molecular geometry is strongly distorted with C-atom hybridization shifting close to sp^3 ($\sim sp^3$) [35]. The C_2H_2 molecule is bound with the surface in the di-σ configuration [35] and its heat of adsorption amounts to ca. –27 kcal/mol [37]. Vattuone *et al.* [37] have also measured a value of ca. –10 kcal/mol and have suggested that this value corresponds to the heat of adsorption of C_2H_2 in the π configuration on Pd(100). The vibrational frequencies of the C—H and C—C stretching modes are 2920 cm^{-1} and 1210 cm^{-1} respectively [35].

The properties of the C_2H_2 molecule on Pd(100) calculated in this work are presented in Table 3. The same tendency as that observed for the adsorption on PdSn(100) and PdPb(100) can be seen in the d values describing the C_2H_2 molecule on Pd(100). The adsorbate molecule sits close to the surface at the hollow site, whereas the distance between the molecule and the surface is the largest for the atop site. The d values, growing in the sequence hollow < bridge < atop, correlate with the increasing Δz values. The calculated bond lengths and angles indicate that the C_2H_2 molecule undergoes some structural changes on the surface. Because of the finite number of atoms in the cluster representing the Pd(100) surface, the C_2H_2 molecule adsorbed at the bridge and hollow sites is not symmetric and thus there are two values of R(C—H) and $\angle$(C—C—H) in Table 3. The $\delta_{C—C}$ and $\delta_{C—C—H}$ values of the

T a b l e 3

Structural, electronic, and vibrational properties of the acetylene molecule adsorbed at the characteristic sites on the Pd(100) *surface. See the caption of Table 1 for further notes*

Property	Adsorption site			Property	Adsorption site		
	atop	bridge	hollow		atop	bridge	hollow
d, Å	2.489	1.939	1.489	$\delta_{C—C—H}$, deg.	14.2	45.3	58.3
	(2.475)	(1.850)	(1.464)			46.6	58.7
$\angle$(C—C—surface), deg.	0.0	4.1	0.9		(7.9)	(45.4	(58.0
	(0.0)	(0.2)	(0.2)			46.3)	58.4)
R(C—C), Å	1.222	1.299	1.351	Q_{MPA}, e	0.2235	–0.0489	–0.2868
	(1.212)	(1.299)	(1.353)		(0.2517)	(–0.0646)	(–0.2846)
R(C—H), Å	1.065	1.086	1.096	Q_{NPA}, e	–0.0455	–0.2620	–0.4587
		1.087	1.097		(0.1449)	(–0.0562)	(–0.1903)
	(1.063)	(1.086	(1.095	v(C—H) sym, cm^{-1}	3364	3071	2956
		1.086)	1.096)		(3388)	(3075)	(2961)
$\angle$(C—C—H), deg.	165.8	134.7	121.7	v(C—H) asym, cm^{-1}	3285	3035	2932
		133.4	121.3		(3301)	(3039)	(2936)
	(172.1)	(134.6	(122.0	v(C—C), cm^{-1}	1862	1533	1363
		133.7)	121.6)		(1919)	(1534)	(1360)
$\delta_{C—C}$, Å	0.023	0.100	0.152	Δz, Å	0.246	0.202	0.085
	(0.013)	(0.100)	(0.154)		(0.000)	(0.000)	(0.000)

C_2H_2 molecule adsorbed at the bridge and hollow sites correspond to the experimental findings of the considerable distortion of the C_2H_2 geometry in the di-σ configuration [35]. The largest values of δ_{C-C} and δ_{C-C-H} can be found for the hollow site and these values reflect the rehybridization of the C atoms from sp to $\sim sp^2$ (according to δ_{C-C-H}) or even slightly over sp^2 (according to δ_{C-C}). The C—C bond length for the C_2H_2 molecule increases from 1.199 Å in the gas phase to 1.351 Å when acetylene adsorbs at the hollow site on the partially relaxed Pd(100) surface. An elongation of the C—C bond to 1.34 Å has been reported for the 3-fold hollow site on Pd(111) [16]. Obviously, the hollow site on Pd(100) is a 4-fold site and, therefore, the slightly longer C—C bond is observed. Based on the experimental ν(C—H) value of 2920 cm^{-1}, Kesmodel [35] has proposed a highly perturbed structure of the C_2H_2 molecule on Pd(100) with its hybridization reaching $\sim sp^3$. Our calculated frequencies of the symmetric and asymmetric C—H stretching modes at the hollow site are in very good agreement with the experiment. On the other hand, the DFT calculations overestimate the ν(C—C) value of C_2H_2 adsorbed at this site by 150—153 cm^{-1}, which means that they predict a somewhat less distorted (and thus stronger) C—C bond with respect to the experimental result. The adsorption at the hollow site is accompanied by a significant electron charge transfer with the dominating role of back-donation.

The C_2H_2 molecule bound with the Pd(100) surface in the di-σ configurations, i.e., at the bridge and hollow sites, exhibits a highly perturbed geometry. The same can be observed for the acetylene structure on the Sn- or Pb-doped Pd(100) surfaces. The adsorption in the π configuration, i.e., at the atop site, leads to a considerably smaller distortion of the acetylene geometry. The structure of the C_2H_2 molecule at the atop-I and atop-II sites on PdSn(100) and PdPb(100) also undergoes a small change compared to that in the di-σ configurations. Obviously, there are some differences between the values of the structural properties of acetylene adsorbed at a given site on monometallic Pd(100) and on doped Pd(100), but these differences are rather minor. It means that, in general, the adsorbate structure on PdSn(100) and PdPb(100) remains similar to that on Pd(100), which is in line with some experimental and theoretical results reported for other surfaces and second metals. C_2H_2 is strongly rehybridized towards $\sim sp^3$ on Pd/Mo(100), as it is on the Pd(100) surface [36]. A very small effect of the second metal on the structure of adsorbed acetylene has been detected for the Pd(111) surface doped with Ag [16]. The lack of significant structural differences between the adsorbates on Pd surfaces versus doped Pd surfaces is not limited only to acetylene. Hill *et al.* [29] have found that the geometry of adsorbed ethylene is similar on Pd(111) and PdSn(111).

It is difficult to find a general trend in the structural changes induced by the two considered dopants. On the one hand, the distortion of the acetylene structure at the hollow-II site on both doped surfaces is smaller than that at the hollow site on Pd(100). On the other hand, the geometry of the C_2H_2 molecule adsorbed at the bridge-I site is perturbed more than that at the bridge site on Pd(100). Similarly, the δ_{C-C} and δ_{C-C-H} values for the atop-I site on PdSn(100) and PdPb(100) are somewhat greater than those at the atop site. In the case of the hollow-I site, the Sn dopant increases the C_2H_2 distortion, whereas the Pb dopant decreases it compared to the C_2H_2 distortion at the hollow site on Pd(100). It is worth noting that the effect of the Pb dopant on the elongation of the C—C bond (δ_{C-C}) is essentially the same for PdPb(100) and PdPb(111) [21].

The analysis of the vibrational frequencies shows that the C—C bond is slightly stronger for the hollow-I and hollow-II sites on PdSn(100) and PdPb(100) than that for the hollow site on Pd(100), and the differences between the ν(C—C) values for the hollow-I/hollow-II site and the hollow site span the range from 17 cm^{-1} to 110 cm^{-1}. Even smaller differences exist between the ν(C—H) values for these sites: –17 cm^{-1} to 67 cm^{-1}.

CONCLUSIONS

The calculations of some structural, electronic, and vibrational properties of the C_2H_2 molecule adsorbed at various sites on the Pd(100) surface doped with Sn or Pb were carried out using the B3LYP hybrid density functional and a cluster model approach. This work reports the C_2H_2 properties on the Sn- or Pb-doped Pd(100) surfaces probably for the first time.

It is found that the geometry of the C_2H_2 molecule adsorbed on PdSn(100) and PdPb(100) in the di-σ configurations, i.e., at the bridge-I, bridge-II, hollow-I, and hollow-II sites, is highly perturbed with respect to the structure of acetylene in the gas phase. It is accompanied by the rehybridization of the C atoms from *sp* to *sp*^{2}. The geometry of acetylene adsorbed on the doped surfaces in the π configurations, i.e., at the atop-I and atop-II sites, shows a much smaller distortion.

The properties of acetylene adsorbed on PdSn(100) and PdPb(100) were also compared with those of C_2H_2 on the monometallic Pd(100) surface in order to establish the effect of the dopant atoms on them. The results indicate that, in general, the geometry of the adsorbed C_2H_2 molecule is similar on the doped and monometallic Pd(100) surfaces. We did not find any trend in the structural changes in acetylene induced by the dopants atoms that is common to all the considered adsorption sites.

REFERENCES

1. *Rylander P.N.* Hydrogenation Methods. – UK, London: Academic Press, 1985.
2. *Molnár Á., Sárkány A., Varga M.* // J. Mol. Catal. A: Chem. – 2001. – **173**, N 1-2. – P. 185 – 221.
3. *Olah G.A., Molnár Á.* Hydrocarbon Chemistry. – US, New Jersey: John Wiley & Sons, 2003.
4. *Brown M.W., Penlidis A., Sullivan G.* // Can. J. Chem. Eng. – 1991. – **69**, N 1. – P. 152 – 164.
5. *Jin Y., Datye A.K., Rightor E. et al.* // J. Catal. – 2001. – **203**, N 2. – P. 292 – 306.
6. *Aduriz H.R., Bodnariuk P., Coq B. et al.* // J. Catal. – 1991. – **129**, N 1. – P. 47 – 57.
7. *Choi S.H., Lee J.S.* // J. Catal. – 2000. – **193**, N 2. – P. 176 – 185.
8. *Palczewska W., Jabłoński A., Kaszkur Z.* // J. Mol. Catal. – 1984. – **25**, N 1-3. – P. 307 – 316.
9. *Sandoval V.H., Girola C.E.* // Appl. Catal. A: Gen. – 1996. – **148**, N 1. – P. 81 – 96.
10. *Volpe M.A., Rodriguez P., Girola C.E.* // Catal. Lett. – 1999. – **61**, N 1-2. – P. 27 – 32.
11. *Nascimento M.A.C.* Theoretical Aspects of Heterogeneous Catalysis. – US, New York: Kluwer, 2001.
12. *Van Santen R.A., Neurock M.* Molecular Heterogeneous Catalysis. A Conceptual and Computational Approach. – DE, Weinheim: Wiley, 2006.
13. *Sellers H.* // J. Phys. Chem. – 1990. – **94**, N 21. – P. 8329 – 8333.
14. *Medlin J.W., Allendorf M.D.* // J. Phys. Chem. B. – 2003. – **107**, N 1. – P. 217 – 223.
15. *Mittendorfer F., Thomazeau C., Raybaud P. et al.* // J. Phys. Chem. B. – 2003. – **107**, N 44. – P. 12287 – 12295.
16. *Sheth P.A., Neurock M., Smith C.M.* // J. Phys. Chem. B. – 2005. – **109**, N 25. – P. 12449 – 12466.
17. *Studt F., Abild-Pedersen F., Bligaard T. et al.* // Angew. Chem. Int. Ed. – 2008. – **47**, N 48. – P. 9299 – 9302.
18. *Nørskov J.K., Abild-Pedersen F., Studt F. et al.* // Proc. Natl. Acad. Sci. – 2011. – **108**, N 3. – P. 937 – 943.
19. *Duca D., Barone G., Varga Z. et al.* // J. Mol. Struct. (Theochem). – 2001. – **542**, N 1-3. – P. 207 – 214.
20. *Ferullo R.M., Touroude R., Castellani N.J.* // Surf. Rev. Lett. – 1997. – **4**, N 4. – P. 621 – 628.
21. *García-Mota M., Gómez-Díaz J., Novell-Leruth G. et al.* // Theor. Chem. Acc. – 2011. – **128**, N 4-6. – P. 663 – 673.
22. *Frisch M.J., Trucks G.W., Schlegel H.B. et al.* Gaussian 09, Revision A.02. – Gaussian, Inc., Wallingford CT, 2009.
23. *Becke A.D.* // J. Chem. Phys. – 1993. – **98**, N 7. – P. 5648 – 5652.
24. *Roy L.E., Hay P.J., Martin R.L.* // J. Chem. Theory Comput. – 2008. – **4**, N 7. – P. 1029 – 1031.
25. *McLean A.D., Chandler G.S.* // J. Chem. Phys. – 1980. – **72**, N 10. – P. 5639 – 5648.
26. *Ehlers A.W., Bohme M., Dapprich S. et al.* // Chem. Phys. Lett. – 1993. – **208**, N 1-2. – P. 111 – 114.
27. *Hay P.J., Wadt W.R.* // J. Chem. Phys. – 1985. – **82**, N 1. – P. 299 – 310.
28. *Bernardo C.G.P.M., Gomes J.A.N.F.* // J. Mol. Struct. (Theochem). – 2001. – **542**, N 1-3. – P. 263 – 271.
29. *Hill J.M., Shen J., Watwe R.M. et al.* // Langmuir. – 2000. – **16**, N 5. – P. 2213 – 2219.
30. *Andersson M.P., Uvdal P.* // J. Phys. Chem. A. – 2005. – **109**, N 12. – P. 2937 – 2941.
31. *Mulliken R.S.* // J. Chem. Phys. – 1955. – **23**, N 10. – P. 1833 – 1840.
32. *Glendening E.D., Reed A.E., Carpenter J.E. et al.* Gaussian NBO Version 3.1. – 2004.
33. *Dewar M.J.S.* // Bull. Soc. Chim. Fr. – 1951. – **18**. – P. C71 – C79.
34. *Chatt J., Duncanson L.A.* // J. Chem. Soc. – 1953. – P. 2939 – 2947.
35. *Kesmodel L.L.* // J. Chem. Phys. – 1983. – **79**, N 9. – P. 4646 – 4648.
36. *Heitzinger J.M., Gebhard S.C., Koel B.E.* // J. Phys. Chem. – 1993. – **97**, N 20. – P. 5327 – 5332.
37. *Vattuone L., Yeo Y.Y., Kose R. et al.* // Surf. Sci. – 2000. – **447**, N 1-3. – P. 1 – 14.